Science Advances
AAAS

Supplementary Materials for

Gamma oscillation plasticity is mediated via parvalbumin interneurons

Michael D. Hadler *et al.*

Corresponding author: Michael D. Hadler, michael.hadler@charite.de; Jörg R. P. Geiger, joerg.geiger@charite.de

Sci. Adv. **10**, eadj7427 (2023)
DOI: 10.1126/sciadv.adj7427

This PDF file includes:

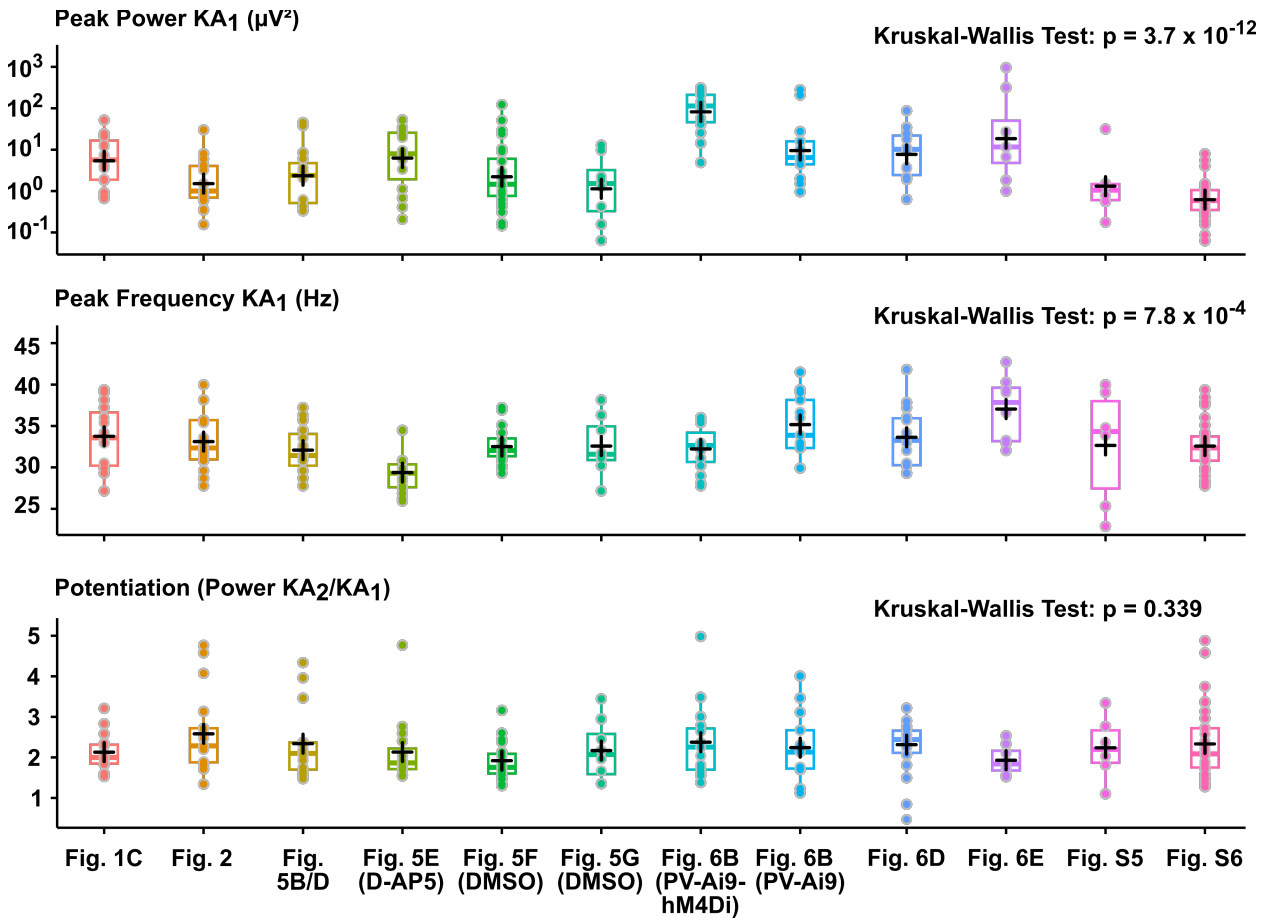

Fig. S1. Multi-trial stability of gamma-potentiation in LFP recordings. Boxplots of all control experiments in the twelve interventions reported. Crosses denote the mean. Above: Log-scale boxplot of peak gamma-power in the first induction period (KA_1). Centre: Peak frequency of oscillations in the first induction period. Below: Magnitude of gamma potentiation. Note the high variability of KA_1 peak power and frequency amongst trials, which is not mirrored in the subsequent potentiation of peak power.

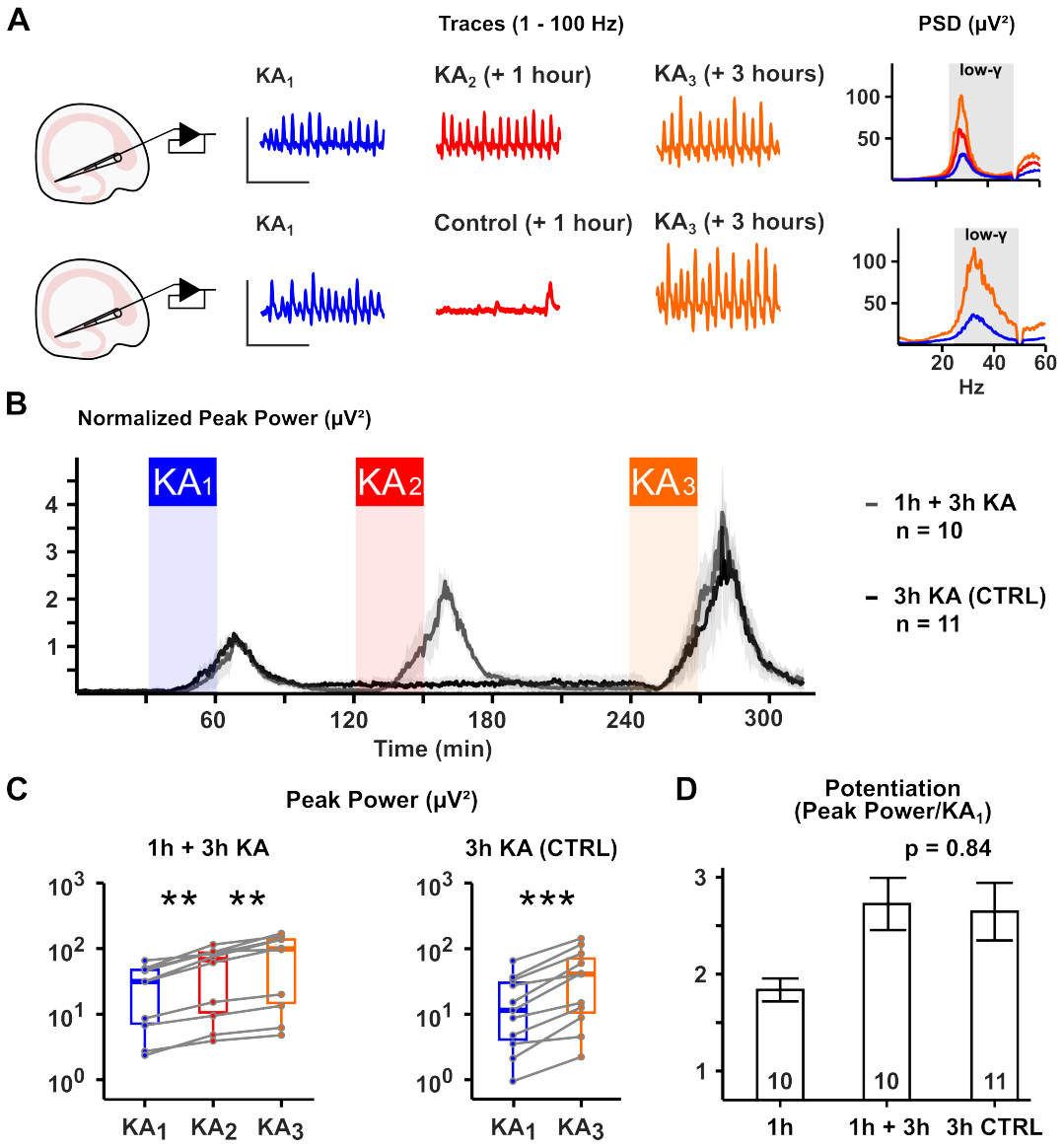

Fig. S2 Long-term saturation of gamma-potentiation. (A) Schematic of the experimental paradigm. All slices are stimulated identically with KA in the first induction period (KA_1), yielding persistent gamma-activity. Slices are subsequently divided into a group receiving two further, identical treatments with KA after 1 hour (KA_2) and 3 hours (KA_3) and a control group receiving just the second additional treatment after 3 hours (KA_3). Spectrograms are obtained and analyzed from all three induction periods. Scales indicate 500 µV/250 ms. **(B)** Time-Power plot of peak power (15 – 49 Hz) for both groups normalized to the first application period. Ribbons denote the 95% confidence interval. **(C)** Paired boxplots of peak gamma-power in both application periods with either 1- and/or 3-hour delay. ** and *** denote $p < 0.01$ and < 0.001, respectively (Wilcoxon signed-rank test). **(D)** Barplot of average potentiation for each application cycle in both groups. P-value in barplot obtained from a log-linked gamma-GLM with post-hoc comparison of estimated marginal means.

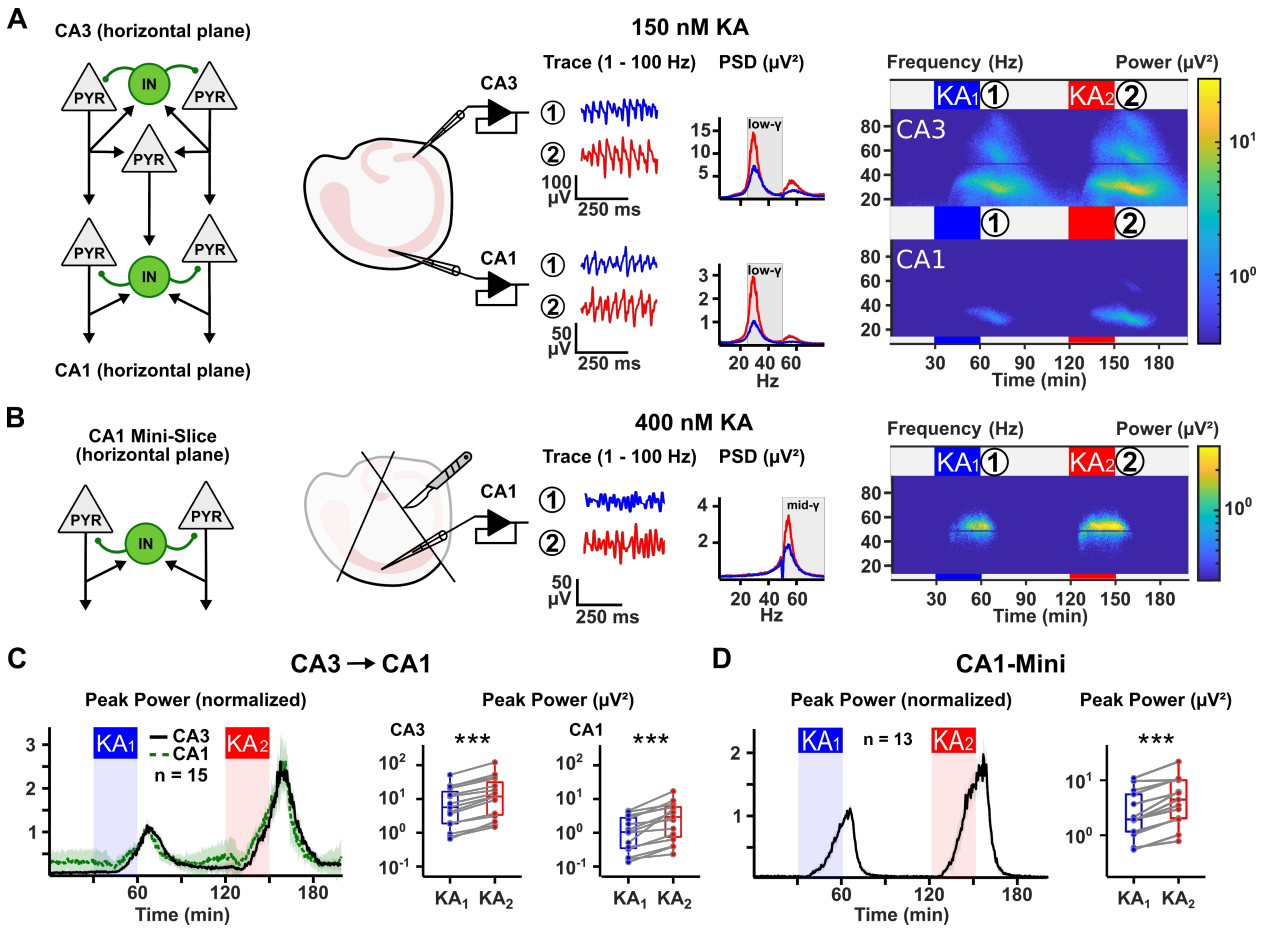

Fig. S3. Gamma-potentiation in paired CA3-CA1 and CA1-Mini LFP recordings. (A) *Left*: Schematic of CA3 and CA1 connectivity in the horizontal slice plane. CA3 pyramidal cells (PYR) are interconnected amongst themselves and local interneurons (INs) and target CA1 PYRs and INs via the Schaffer collateral pathway. CA1 PYRs do not connect amongst each other but are interconnected with local CA1 INs. *Centre*: Schematic of a hippocampal slice with LFP electrodes in CA3 and CA1. Exemplary traces as in Fig. 1A with simultaneous recordings of CA3 and CA1. *Right*: Pseudocolor plots of the entire experiment. **(B)** *Left*: Schematic of the CA1 Mini-slice microcircuit. *Centre*: Schematic drawing of the hippocampus with surgical cuts separating CA1 from the subiculum and CA3. A recording pipette was placed in stratum pyramidale. *Right*: Same as in (A) but for an exemplary recording in a CA1-Mini slice. Gamma-activity was induced with 400 nM KA instead of 150 nM. Grey inset "mid-gamma" in the PSDs denotes the window spanning 50 – 80 Hz. **(C)** *Left:* Time-Power plot for all paired CA3-CA1 recordings normalized to the first induction period. *Right:* Paired boxplots of peak gamma-power in both application periods in CA3 and CA1. **(D)** Same as (C), but for the experiments in CA1-Mini slices. *** denotes $p < 0.001$ (Wilcoxon Signed-Rank test).

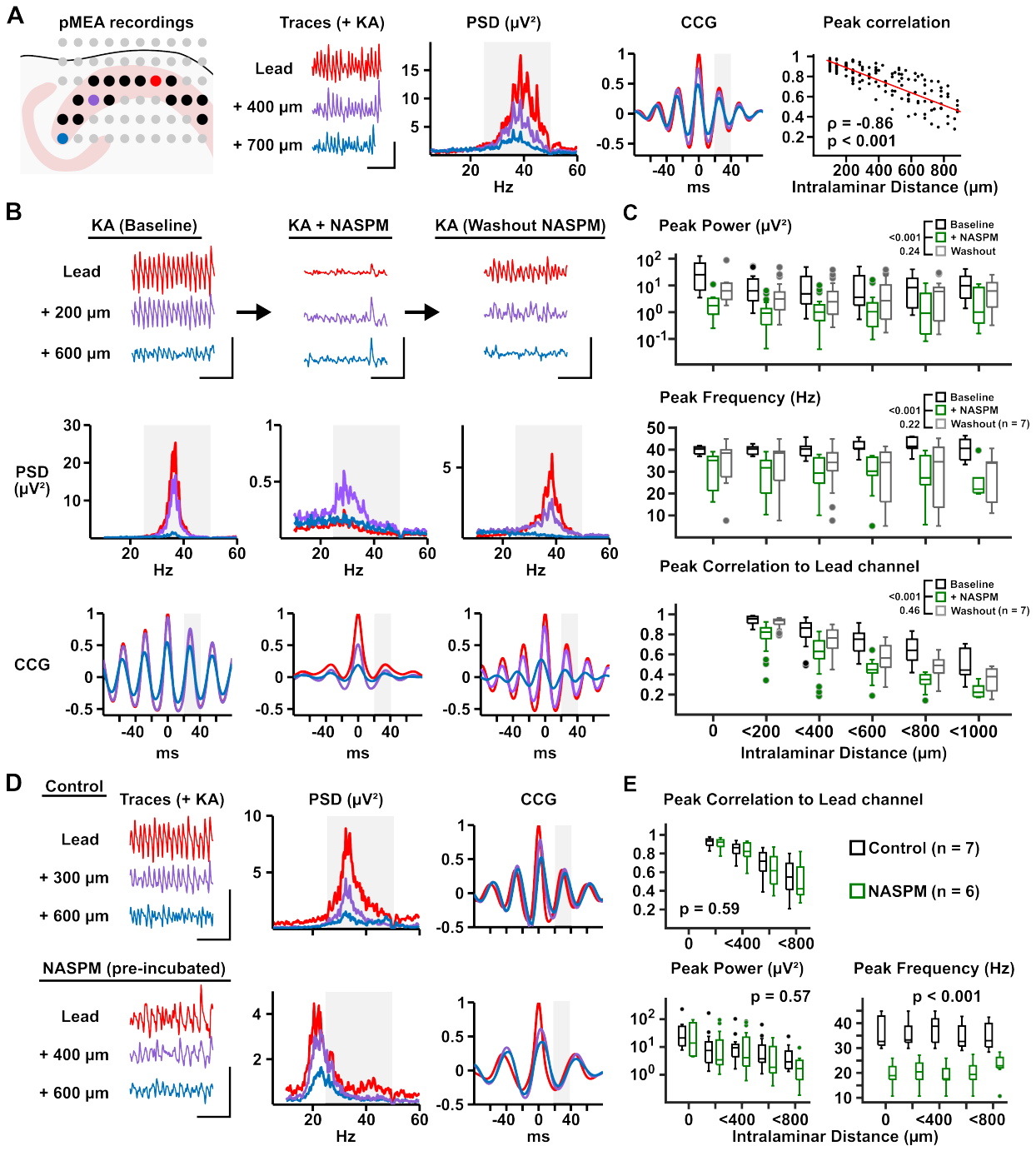

Fig. S4. CP-AMPARs generate and maintain the gamma-rhythm in pMEA recordings. (A) Gamma-oscillations are generated across CA3 with decreasing inter-site cross-correlation. *Left, Centre*: Exemplary recording configuration in the 6 x 10 MEA grid with selected electrodes in black. Red, purple and blue electrodes resemble the recordings displayed in the traces, PSDs and cross-correlograms (CCG) after application of KA (200 nM). The red correlogram represents the auto-correlogram of the "lead electrode" (highest power in PSD). *Right*: Scatter plot of pooled peak cross-correlation of electrodes to the lead electrode. A linear fit is superimposed. Rho and p refer to the results of Pearson's correlation test. **(B)** Gamma-oscillations are maintained by CP-

AMPARs. An exemplary experiment with traces at three sites (above) and the corresponding PSDs (centre) and correlograms (below). After an initial induction of gamma-oscillations with 200 nM KA (left), NASPM is added to the bath (centre) and oscillations dissipate. Following washout of NASPM (right), oscillations re-appear in 2/3 sites displayed. **(C)** Boxplots to the experiments in (B). Values are displayed for peak power, frequency and cross-correlation as a function of intralaminar distance. P-values refer to group comparisons towards baseline (generalized linear model). Peak power values were log-transformed before statistical testing. **(D)** CP-AMPAR lacking rhythms are similar to gamma-oscillations in power and inter-site cross-correlation, but markedly reduced in peak frequency. Exemplary experiments as in (B) for a control slice (above) and a slice pre-incubated with NASPM (100 µM) before application of KA (200 nM). In the presence of NASPM, the peak of the PSD and correlograms is clearly below the low gamma-frequency range (25 – 50 Hz and 20 – 40 ms for PSD and correlograms, respectively). **(E)** Boxplots of recorded peak values for power, frequency and cross-correlation to the lead channel as a function of intralaminar distance toward the lead channel. A reduction in peak frequency is observed across all recording sites after pre-incubation with NASPM. P-Values obtained from a generalized linear model.

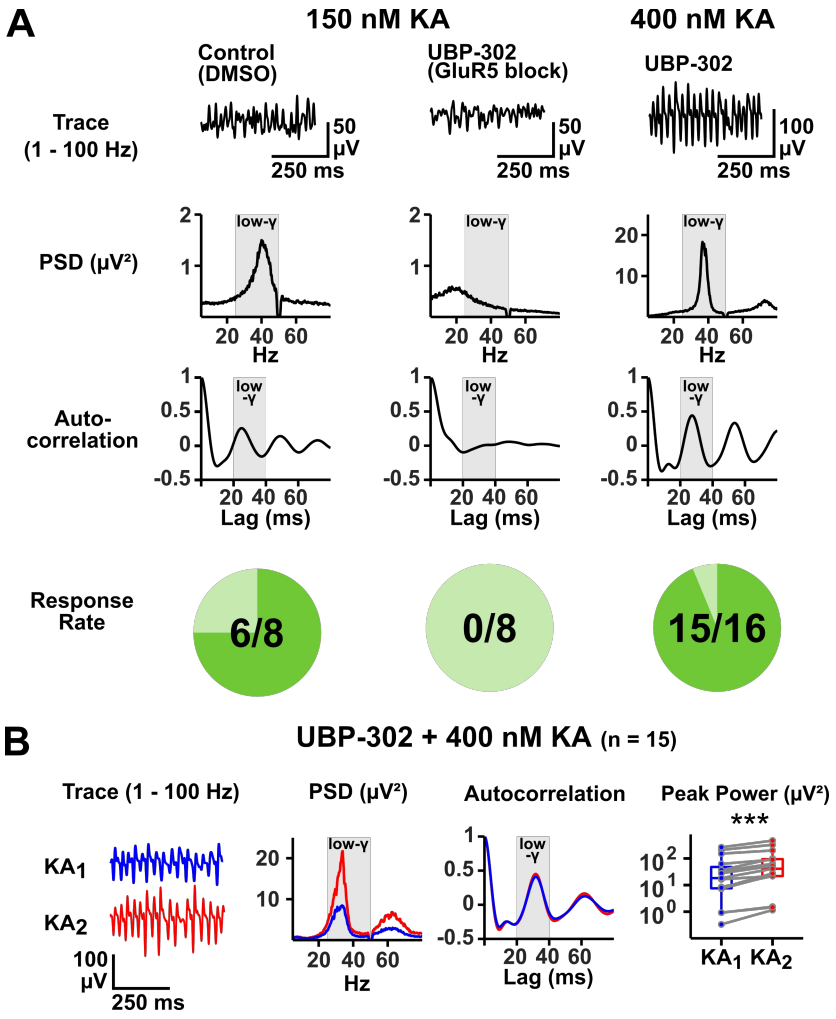

Fig. S5. Blockade of GluK1 with UBP-302 attenuates the induction of gamma-oscillations but does not alter gamma-potentiation. (A) Exemplary traces, power spectra and ACGs for DMSO Control experiments and UBP-302 pre-incubation with two concentrations of KA (150 and 400 nM). At 150 nM KA, pre-incubation with UBP-302 prevents the generation of a discernible rhythm in the ACG. Below: Pie charts of the response rates of the individual paradigms. **(B)** Gamma-potentiation in the presence of UBP-302 at 400 nM KA. *Left*: Exemplary traces during the first and second induction period (KA_1 and KA_2). *Centre*: Corresponding PSD and ACG. Grey insets "low-gamma" in the PSDs and ACGs denotes the window spanning 25 – 50 Hz. *Right*: Paired boxplot of peak gamma-power during both induction periods. *** denotes $p < 0.001$ (Wilcoxon Signed-Rank test).

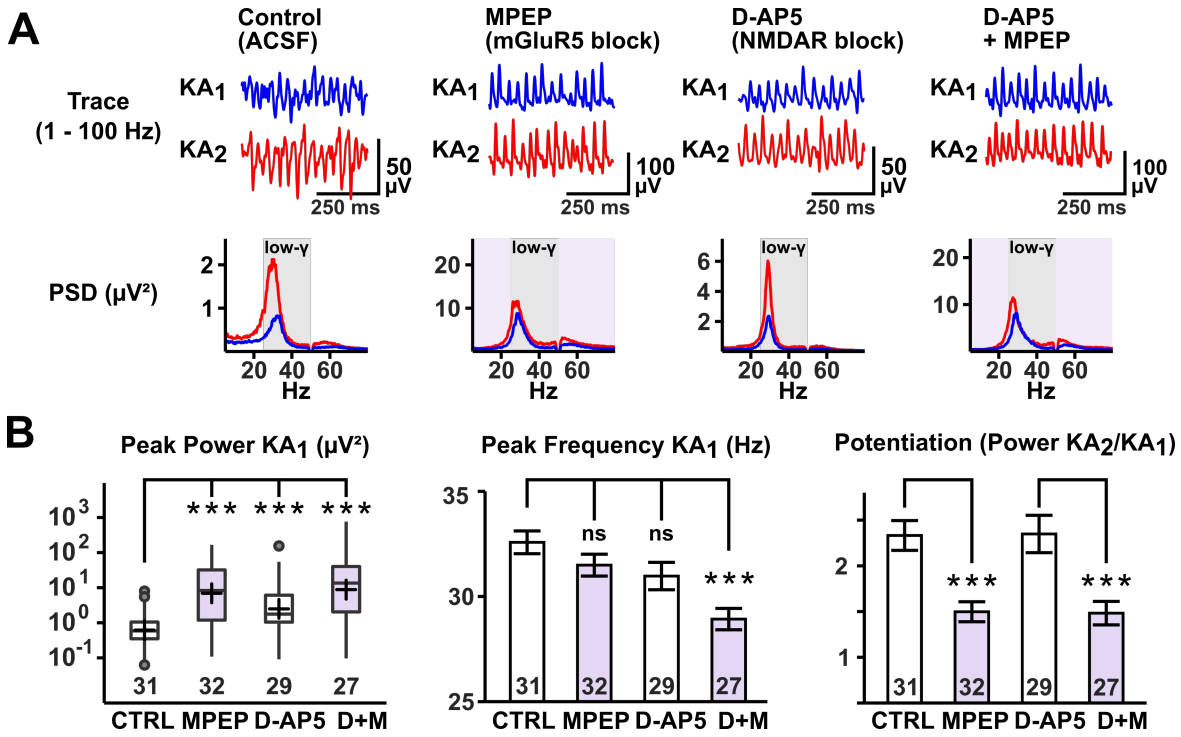

Fig. S6. mGluR5, not NMDARs, contributes to gamma-potentiation. Blockade of NMDARs and mGluR5 increases peak gamma-power and decreases peak gamma-frequency. (A) Exemplary traces and power spectra for Control, D-AP5, MPEP and D-AP5 + MPEP (D+M) conditions during both induction periods (KA_1, KA_2). **(B)** Summary statistics for all conditions. *Left*: Boxplot of peak gamma-power in KA_1 for all conditions. *** indicates $p < 0.001$, multiple Mann-Whitney U-tests. *Centre*: Barplot of peak gamma-frequency during KA_1. *Right*: Barplot of potentiation of peak power in all conditions. *** and ns in barplots denote $p < 0.001$ and $p > 0.05$ (generalized linear model). Purple insets denote the application of MPEP.

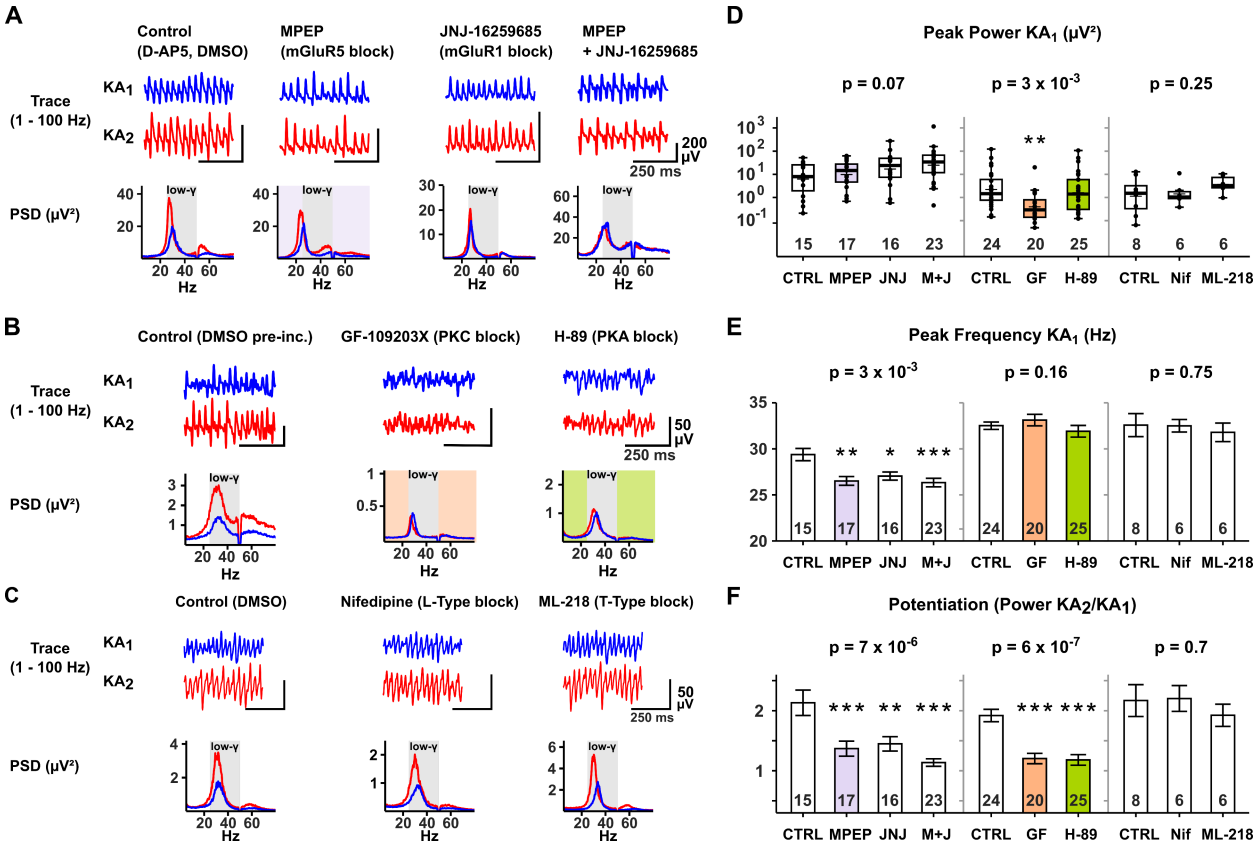

Fig. S7. Contribution of mediators of synaptic plasticity towards induction and plasticity of gamma oscillations. (A-C) Exemplary traces and PSDs for data presented in Fig. 5E-G. **(D)** Boxplots of peak gamma power in the first induction period (KA_1) in all three studies. Blockade of PKC with GF 109203X (3 µM) reduces peak gamma power. **(E)** Barplot of average peak frequencies in KA_1. Blockade of either mGluR5 with MPEP (10 µM) or JNJ-16259685 (0.3 µM) or both substances reduces the peak frequency. **(F)** Barplots of average potentiation as shown in Fig. 5E-G. P-values in plots indicate the result of the Kruskal-Wallis test in the respective study. *, ** and *** indicate $p < 0.05$, 0.01 and 0.001 (Mann-Whitney U-test in (D), generalized linear models in (E-F)).

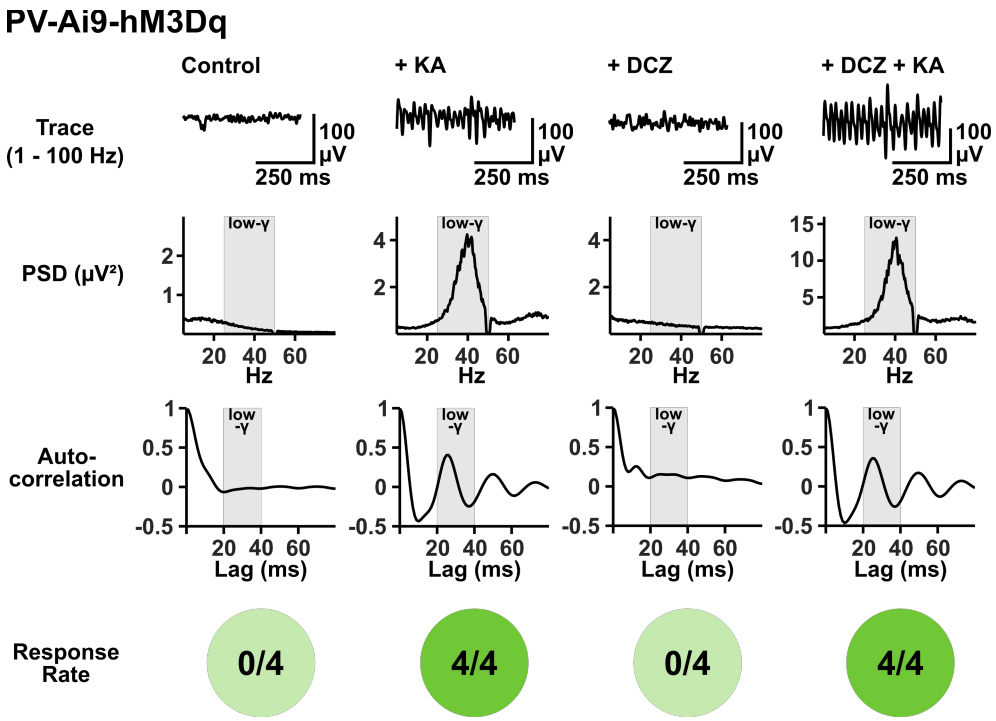

Fig. S8. Sole activation of hM3Dq in PVIs is insufficient to synchronize CA3 network activity. Traces, PSDs and ACGs of conditions testing whether gamma-activity can be induced with just 3 µM DCZ as compared to application of kainate (KA, 150 nM). Pie charts below indicate the numbers of slices in which oscillations were induced for each condition. KA or DCZ were applied or co-applied for 30 minutes.

Table S1. Passive parameters and active conductance values for all compartments of the pyramidal model cell.

Mechanism	***Soma***	***Proximal Apical Dendrite***	***Distal Apical Dendrites***	***Basal Dendrites***
Leak conductance [S/cm^2]	0,0002	0,0002	0,0002	0,0002
Na^+ conductance [S/cm^2]	0,0105	0,0084	0,0084	0,0084
Delayed rectifier K+ conductance [S/cm^2]	0,00086	0,00086	0,00086	0,00086
Proximal A-type K+ conductance [S/cm^2]	0,0075	0,015	-	0,0075
Distal A-type K+ conductance [S/cm^2]	-	-	0,04875	-
M-type K+ conductance [S/cm^2]	0.06	0.06	-	0.06
Ih conductance [S/cm^2]	0.00005	0.0001	-	0.00005
L-type Ca2+ conductance [S/cm^2]	0.0007	0.00003	-	0.00003
R-type Ca2+ conductance [S/cm^2]	0.0003	0.00003	-	-
T-type Ca2+ conductance [S/cm^2]	0.00005	0.0001	-	0.0001
Ca^{2+}-dependent sAHP K^+ conductance [S/cm^2]	0.0015	0.001	-	0.0005
Ca^{2+}-dependent mAHP K^+ conductance [S/cm^2]	0,9	0,03	-	0,08
Membrane capacitance Cm [µF/cm^2]	1	1	1	1
Membrane resistance Rm [Ohm cm^2]	6000	6000	6000	6000
Axial resistance Ra [Ohm cm]	150	150	150	150

Table S2. Electrophysiological characterization of the pyramidal model cell.

Parameter	***Value***
Rheobase (pA)	200
Input Resistance (MΩ)	142
Spike Threshold (mV)	-43,11
Spike Amplitude (mV)	73,11
Spike Overshoot (mV)	30
Resting Membrane Potential (mV)	-70
AP Frequency (Hz) during Rheobase current clamp	6

Table S3. CA3 microcircuit synaptic conductance values.

Synapse Type	*Pyramidal model*	*PV Basket Cell model*
INPUT AMPA	0,002	-
INPUT NMDA	0,005	-
CI-AMPA	0,0017 (baseline) 0,00255 (plasticity)	-
CP-AMPA	-	0,0015 (baseline) 0,00225 (plasticity)
NMDA	0,0051	0,0016
GABA	0,004	0,005
Autapse GABA	-	0,007